RESEARCH ARTICLE | MAY 31 2018

Modelling of structure and dynamics of molten NaF using first principles molecular dynamics FREE

Sanghamitra Mukhopadhyay ✉; Franz Demmel

AIP Conf. Proc. 1969, 030001 (2018)
https://doi.org/10.1063/1.5039293

Modelling of Structure and Dynamics of Molten NaF using First Principles Molecular Dynamics

Sanghamitra Mukhopadhyay[a)] and Franz Demmel[b)]

ISIS Neutron and Muon Source Facility, Rutherford Appleton Laboratory, Science and Technology Facility Council, Harwell Science and Innovation Campus, Didcot, Oxfordshire OX10 0QX, United Kingdom

[a)]Corresponding author: sanghamitra.mukhopadhyay@stfc.ac.uk
[b)]franz.demmel@stfc.ac.uk

Abstract. Some aspects of the microscopic structure and dynamics in molten NaF are presented by first principles MD simulations. From distribution plots of NaF inter-ionic distances, F-Na-F angles and local coordination numbers of the melt structure have been studied. The analysis of coordination numbers shows that most of the Na or F are surrounded by four to five ions of opposite polarity. This is different from their solid state form, where octahedral environment is expected for each ion. The dynamical properties of molten NaF are investigated through the self-intermediate scattering function I(Q,t). The calculated I(Q,t) compares well with the experimental one obtained through Fourier transformation. The power spectrum of the velocity autocorrelation function from the MD simulation allows to obtain partial density of states of molten NaF, which links diffusive motions with the vibrational density of states. The short, medium and long time motion of molten NaF is discussed on the basis of these calculations.

INTRODUCTION

Applications of quasielastic neutron scattering (QENS) relies on its analysis which is traditionally done by fitting neutron spectra with several empirical functions based on analytical models. Although these models work up to a certain extent, their applicability is limited. To overcome this limitation atomistic simulations using molecular dynamics (MD) are performed. The classical force field based MD requires well-defined empirical models of interatomic forces which are not available for complex chemical environment and extreme conditions, such as high temperatures, pressures, presence of surfaces, defects or impurities. With the increase of the capability of neutron scattering instruments and sophisticated sample environment facilities, modern QENS experiments are performed on complex chemical systems in those challenging situations. In this perspective application of parameter-free first principles MD is a way forward to understand the dynamics of complex materials in the analysis of QENS spectroscopy.

For example, molten salts are ionic liquids at high temperatures. Due to their large heat capacities, large ionic conductivities at high temperatures and stability for a large liquid temperature range, salts find industrial applications as heat storage in modern solar power plants, in next generation nuclear reactors and in extractions of metals from ores [1, 2, 3]. Many electrochemical processes are dependent on ion conductivity and hence an understanding of the diffusivity of the individual ions in the melt is important [4, 5, 6]. A microscopic model of molten salts can be assumed as a random network of charged particles with charge ordering due to the long range Coulomb interaction. Being the most simple class of molten salts molten alkali halides attract a lot of attention both from experimental and computational scientists [7, 8].

Due to the conceptual simplicity classical rigid ion models are used since decades to model structural and dynamical properties of molten alkali halides [9, 10]. Although these models work for the prediction of spatial distribution of ions, the effect of polarisation becomes important to calculate dynamical properties, particularly the diffusivity of cations [11, 12, 13, 14, 15]. Finding out force fields suitable for predicting ionic dynamics at high temperatures as well as having transferability is challenging. To address this challenge, first principles-DFT based calculations have been used to extract more advanced interaction potentials, e.g. [3, 16, 17, 18, 19, 20].

Understanding structure and dynamics on a microscopic level is the main driving force of neutron spectroscopy. However, there are not so many studies in this area on molten salts. This is partly due to the low scattering cross

Proceedings of the Joint Conference on Quasielastic Neutron Scattering and the Workshop on Inelastic Neutron Spectrometers QENS/WINS 2016
AIP Conf. Proc. 1969, 030001-1–030001-7; https://doi.org/10.1063/1.5039293
Published by AIP Publishing. 978-0-7354-1676-5/$30.00

sections of constituent elements and partly because of the demanding experimental conditions [21, 22]. Recently single ion dynamics in molten salts were investigated by quasielastic neutron scattering (QENS) and complemented by classical and first-principles based molecular dynamics (MD) calculations [15, 23]. Due to the progress in computing power it is realistic to do first principles based MD, which doesn't require any empirical parameters for determination of force fields to provide reliable microscopic understanding of neutron spectroscopy [24]. Recent reports on a molten LiCl-KCl mixture, molten NaCl, NaI and NaF are examples of such attempts [23, 25, 26]. Although diffusion coefficients are reported in those work, discussions on local structures and details of microscopic motion are absent.

In the current report we present the result of our microscopic analysis of structure and dynamics through first-principles MD simulations of molten NaF in comparison with results from a QENS experiment [23]. Complementary structural and dynamic details will be presented which are not possible to obtain from an experiment. The calculations are performed within first principles based MD which is free from any adjustable parameters and can be a benchmark for future MD-simulations and experiments. The aim is to shed some light onto the interplay of structure and dynamics in molten NaF on a microscopic level.

Methodology of Calculations

MD simulations have been performed based on first principles DFT using CASTEP code [27] on a supercell consisting of 256 NaF molecules. Periodic boundary condition was applied. The ultrasoft pseudopotentials [28] generated with the Perdew-Burke-Ernzerhof (PBE) [29] functional within the generalized-gradient approximation (GGA) have been used. A plane-wave cut off energy 1000 eV and tolerance for self consistent energy minimisation below $2.5 \cdot 10^{-8}$ eV/ion were used. The NPT ensemble with Nose-Hoover thermostat and Andersen-Hoover barostat were used to stabilize temperature and pressure, respectively. Relaxation times for the thermostat and the cell were specified as 5 ps and 500 ps, respectively. A pressure of 1 bar was kept constant and a MD time step of 2 fs was used all throughout. During simulations the volume of the cell was allowed to change with temperatures by keeping the shape preserved which is suitable for liquid simulations. The mass density during the simulation runs was $\rho = 1.914\ g/cm^3$, very near to the experimental density. The details of the melting process has been reported elsewhere [23]. Production runs have been taken at 1300 K.

The partial pair distribution functions (PDFs) $g_{i,j}(r)$ can be calculated from average density of particles i at a distance r from a tagged particle j at the origin [30]:

$$c_i c_j \rho g_{ij}(r) = \langle \frac{1}{N} \sum_{i=1}^{N_i} \sum_{j=1}^{N_j} \delta(r + r_j - r_i) \rangle \tag{1}$$

where c_i are the number density of particle of type i, ρ the average particle density . The pair distribution function $g_{ij}(r)$ can be deduced from the radial particle distribution:

$$g_{ij}(r) = N_{ij}(r)/[\rho_j 4\pi r^2 dr] \tag{2}$$

where $\rho_j = c_j \rho$ is the particle density of type j, N_{ij} is the number of particles of type j between distances r and r+dr from a particle of type i and dr is the histogram shell width, 1.0×10^{-3} Å in the current calculations.

The incoherent intermediate scattering function $I(Q,t)$ can be calculated from the Fourier components of the microscopic particle density $\rho_Q(t) = e^{iQr_n(t)}$:

$$I_(Q,t) = \langle e^{-i \cdot Q r_n(t)} e^{i \cdot Q r_n(0)} \rangle \tag{3}$$

where the brackets denote a thermal average. The programme package nMoldyn has been utilized for the calculation of the different scattering functions [31].

Since $S(Q,\omega)$ is the Fourier transform of $I(Q,t)$, simulations of long durations are required to get smooth $S(Q,\omega)$ spectra, in particular at small momentum transfers when the decay of the correlations over longer distances are becoming longer. On the other hand a smooth $I(Q,t)$ can be calculated directly from the trajectory of MD simulations of comparatively smaller time durations.

Further neutron observable can be calculated from the MD trajectory is the vibrational densities of states (VDOS). This quantity can be obtained experimentally from inelastic neutron scattering (INS) spectroscopy. VDOS can be calculated from the Fourier-cosine transformation of the time-dependent velocity autocorrelation function (VACF):

$$C_{jj}(t) = (1/3)\langle \overrightarrow{v}_j(t) \overrightarrow{v}_j(0) \rangle \tag{4}$$

where $\overrightarrow{v}_j(t)$ is the velocity of the species j at time t and $C_{jj}(t)$ is a thermal average of the velocity correlation of a tagged particle between time zero and a time t.

Experiments

A QENS experiment was performed on molten NaF at 1300 K at the OSIRIS spectrometer of the ISIS Facility, UK. OSIRIS is an indirect time of flight backscattering spectrometer with final energy of $E_f = 1.845\ meV$ for the PG002 analyser reflection [32]. In this setting the energy resolution is 25 μeV. NaF powder was filled into an electron beam welded cylindrical niobium cell of wall thickness 0.2 mm and diameter 10 mm. This setting provided a scattering power of about 15 %. As a coherent scatterer Niobium contributes only to Debye-Scherrer lines, which are outside the covered momentum range of the PG002 setting. The melting temperature of NaF is 1268 K. More details of the experiment can be found elsewhere [23]. Na is a nuclei with nearly equal coherent and incoherent scattering cross sections and fluorine has no incoherent cross section at all [33]. At small momentum transfers the measured signal is dominated by the incoherent contribution of the Na ions. The intermediate scattering function $I_{Na}(Q,t)$ can be obtained through Fourier transform from the dynamic structure factor $S(Q,\omega)$. In the hydrodynamic limit $I(Q,t)$ is described by a simple exponential decay:

$$I(Q,t) = e^{-Q^2 Dt} \tag{5}$$

From that dependence the diffusion coefficient can be derived directly.

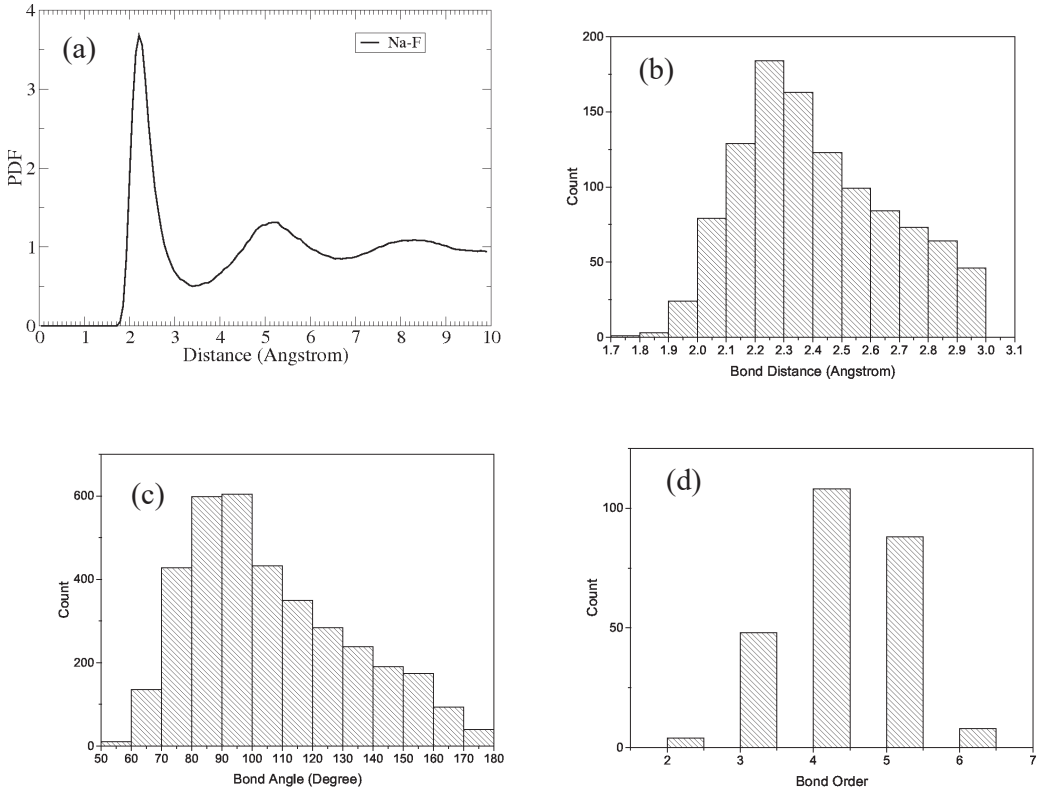

FIGURE 1. Structural properties of molten NaF. (a) PDF of Na-F, (b) distribution of Na-F bond distances, (c) distribution of F-Na-F angles, (d) coordination number of F ions.

Results and Discussion

The structural properties of molten NaF as obtained after 50 ps production run are shown in Fig. 1. The calculated PDF is shown in Fig. 1(a). The absence of long range order in the PDF confirms the liquid state of the simulated cell. The highest peak of the PDF occurs at 2.3 Å corresponding well to the interatomic distances of Na and F ions [34] and the position of the peak in the distribution of NaF distances as shown in Fig.1(b). As expected from calculated PDF this distribution also shows the most probable peak at 2.3 Å. About 32 % of all Na-F bonds are lying between 2.2 – 2.4Å, however, the distribution of bond lengths varies from as small as 1.7 Å to almost 3.0 Å. This finding shows that although there is no long range order in molten NaF, short range order, such as Na-F distance is preserved in the molten state and at temperature of 1300 K. This finding is similar to that of amorphous silica [35], where short range order has been preserved in the amorphous structure.

To investigate the orientational order of the molten salt, the distribution of F-Na-F angle is shown in Fig. 1(c). The peak position of this distribution is at 90^0, however, the value of these bond angles varies widely. About 35 % of all such angles are between $80^0 - 90^0$. A few percentages of bond angles are of 180^0 showing that very few $F - Na - F$ species are linear. This finding is supported further by the coordination number of F ions as presented in Fig.1(d).

The coordination numbers, presented in Fig.1(d), have been calculated by counting cations which are in the sphere of anions within a distance of 3.0 Å. Presence of another F ion in this sphere has not been considered. It is found that most of the F ions are four- to five-fold coordinated rather than octahedral coordinated as expected for a cubic ionic structure. That result agrees with previous structural investigations on molten salts [36, 37, 38, 39]. The four coordinated F ions are present at about 43 % whereas only 4 % are of six coordinated species. Further analysis shows that the four coordinated F ions are not planar with an angle variation for Na-F-Na from 80° − 160°. The Na-F-Na angle in two coordinated F ions is not 180^0 as expected for a linear molecular unit, but vary from 100° − 140°.

The coordination numbers of Na ions are found to be slightly different from that of F ions where is a change in four and five coordinated Na ions. This is due to the different size of the ions. No significant change in the Na-F-Na bond angle has been found. Also no free Na or F ions or isolated dipole is found in the melt.

The structure of a liquid is not static but changes with time and temperatures. This change can be captured through the investigation of its dynamical properties. In the current work a QENS experiment has been employed to understand the microscopic nature of this dynamics. The $S(Q, \omega)$ spectra as obtained from the QENS experiment has been reported before along with the MD simulations [23]. Diffusion constants calculated from the MD-simulations compare well with experiment at the low Q approximation.

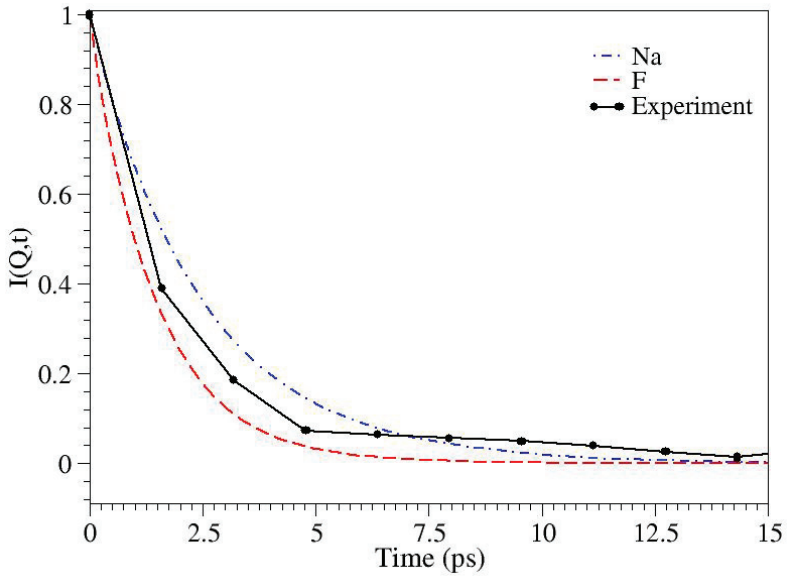

FIGURE 2. Intermediate scattering functions from MD simulations for Q = 0.6 Å^{-1} . Experimental data are shown by symbols. Error bars in the experimental data are less than 10^{-2} and are invisible because their sizes are less than the width of symbols.

The partial intermediate scattering functions of molten NaF as obtained from MD simulations are plotted in Fig.2 for $Q = 0.6$ Å^{-1}. Although a trajectory of 50 ps has been considered in this calculations, it is found that only the first 10 ps are important to understand the dynamics. From the figure it is clear that although Na and F ions decay similarly, the time constants of this decay are slightly different. The diffusion coefficient D can be obtained from the relation $I(Q,t) = exp(-Q^2Dt)$. It is found that the decay of F and Na ions can be fitted with a single exponential functions, which indicates Fick-type diffusion for $Q = 0.6$ Å^{-1} in this melt. The F ions decay faster than Na ions. The faster motion of F ions may be due to its smaller mass, but, it may be due to its change in coordination number with respect to Na as discussed above. In the long time approximation, however, diffusion coefficient of both ions are almost the same. This result is consistent with our previous report on diffusion coefficients of molten NaF [23].

As shown in Fig.2 the calculated I(Q,t) compares well with experiment. The difference in the value of calculated I(Q,t) with that of experiment at times greater than 5 ps may be an artifact of the Fourier transform of the experimental $S(Q,\omega)$ spectra. This artifact may arise due to the small energy transfer range (< 1 meV) in the quasielastic experiment.

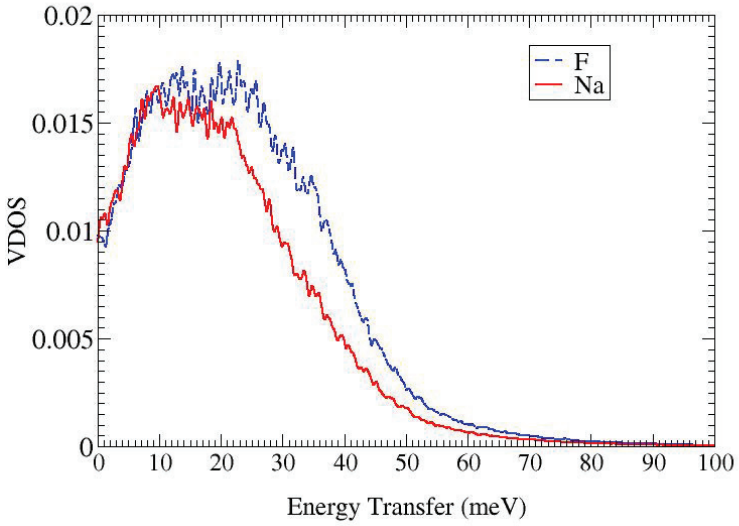

FIGURE 3. Vibrational densities of states (VDOS) of molten NaF calculated using MD simulations.

To investigate further the dynamical processes the power spectrum of the velocity autocorrelation function has been calculated and plotted in Fig. 3. The frequency spectrum of the velocity autocorrelation function is directly linked to the vibrational density of states and here we show the partial vibrational density of states [40]. The maximum of the spectrum occurs at around 25 meV (200 cm^{-1}) and is due to the vibrational dynamics of the ions. The partial contribution of the heavier Na ion is relatively slower and the whole frequency distribution can be found at lower frequencies. It appears that the power spectrum has some structure, which might be related to the vibrational properties of NaF. The shape of the VDOS curve is important to understand the short, medium and long time dynamics of a liquid [41]. Two types of motions determine the shape of the VDOS, the Brownian motion of diffusion and the oscillator motion of individual ions. The very low frequency regime ($\omega \rightarrow 0$) depends on the diffusivity of the liquid, on the other hand for large ω the oscillator nature of the particles is important. The position of two peaks at relatively finite values of ω corresponds to the oscillator strengths of NaF. Lattice dynamics calculations for solid NaF have shown that the vibrational density of states has maxima at about 20 meV (160 cm^{-1}) and a broad band of excitations around 30 meV (240 cm^{-1}) from the van Hove singularities of acoustic and optic modes [42]. That frequency range agrees well with the main maximum of the power spectrum of molten NaF. As a maximum vibrational frequency for the solid NaF 52 meV (420 cm^{-1}) was calculated which agrees well with the higher limit of our calculated frequency spectrum. The calculations of the VDOS depends on accurate descriptions of interatomic forces. Since here the structure and dynamics of molten NaF are obtained by first principles MD simulations, it is free from ambiguous fitting parameters

generally used to get a good force field. Calculated QENS observables compare well with experiments. Thus the current calculation can be a benchmark to get suitable force fields for these ionic melts, which might then be compared to measurements of the vibrational properties [43, 44].

Conclusions

Results from a first principles MD simulations of molten NaF have been presented. The structure of the melt has been analysed from the distribution plot of NaF interionic distances, F-Na-F angles and local coordination number of a particular species. It is found although the Na-F bond distances and angles are preserved in the liquid NaF, both of them have a wide distribution. The analysis of coordination number shows that most of the Na or F are surrounded with four to five other ions of opposite polarity. This is different from their solid state form, where octahedral local coordination is expected for each ions. To investigate further the dynamical property of molten NaF, the intermediate scattering function has been calculated and compared with experiments. It is found that F decays a little bit faster than Na at the first 5 ps, but overall diffusion constants of Na and F are almost the same. The short, medium and long time dynamics are predicted from the power spectrum of the velocity autocorrelation function, which can be probed through inelastic neutron scattering experiments.

ACKNOWLEDGMENTS

We thank the ISIS Facility for the provision of beam time, and the UK Science and Technology Facilities Council e-Science Department for continued access to the SCARF cluster at the Rutherford Appleton Laboratory. Some of the computations have been performed on the UK High Performance Computing Facility HECToR, and ARCHER under the auspices of the Materials Chemistry Consortium (EPSRC grant EP/D504872 and EP/L000202).

REFERENCES

[1] C. LeBrun, J. Nuclear Mat. **360**, p. 1 (2007).
[2] S. Delpech, E. Merle-Lucotte, D. Heuer, M. Allibert, C. L.-B. V. Ghetta, X. Doligez, and G. Picard, Fluorine Chem. **360**, p. 11 (2009).
[3] L. Dewan, C. Simon, P. Madden, L. Hobbs, and M. Salanne, J. Nuclear Mat. **434**, p. 322 (2013).
[4] Z. Akdeniz and P. Madden, J. Phys. Chem **110**, p. 6683 (2006).
[5] S. Jahn, J. Ollivier, and F. Demmel, Solid State Ionics **179**, p. 1957 (2008).
[6] F. Demmel, T. Seydel, and S. Jahn, Solid State Ionics **180**, p. 1257 (2009).
[7] N. March and M. Tosi, *Coulomb Liquids* (Academic Press, San Diego, 1984).
[8] M. Rovere and M. Tosi, Rep. Prog. Phys. **49**, p. 1001 (1986).
[9] G. Ciccotti, G. Jacucci, and I. McDonald, Phys. Rev. A **13**, p. 426 (1976).
[10] O. Alacaraz and J. Trullas, J. Chem Phys **113**, p. 10635 (2000).
[11] M. J. L. Sangster and M. Dixon, Adv. Phys. **25**, p. 247 (1976).
[12] M. Dixon, Phil. Mag. B **47**, p. 509 (1983).
[13] M. Wilson and P. Madden, J. Phys: Condens Matter **6**, p. A151 (1994).
[14] O. Alacaraz, V. Bitrian, and J. Trullas, J. Chem Phys **127**, p. 154508 (2007).
[15] O. Alcaraz, F. Demmel, and J. Trullas, J. Chem Phys **141**, p. 244508 (2014).
[16] R. Heaton, P. Madden, S. Clark, and S.Jahn, J. Chem Phys **125**, p. 14104 (2006).
[17] M. Salanne, R. Vuilleumier, P. Madden, C. Simon, P. Turq, and B. Guillot, J Phys: Condens Matter, **20**, p. 494207 (2008).
[18] M. Salanne and P. Madden, Mol Phys **119**, p. 2299 (2011).
[19] M. Salanne, C. Simon, P. Turq, and P. Madden, J Fluorine Chem **130**, p. 38 (2009).
[20] Y. Ishii, K. Sato, M. Salanne, P. Madden, and N. . Ohtor, J. Phys Chem B **118**, p. 3385 (2014).
[21] R. McGreevy, Solid State Physics **40**, p. 247 (1987).
[22] R. McGreevy, E. Mitchell, and F. Margaca, J Phys C **17**, p. 775 (1984).
[23] F. Demmel and S. Mukhopadhyay, J. Chem Phys **144**, p. 014503 (2016).
[24] S. Mukhopadhyay, M. Gutmann, and F. Fernandez-Alonso, Phys. Chem. Chem. Phys. **16**, p. 26234 (2014).
[25] A. Bengston, H. Nam, S. Saha, R. Sakidja, and D. Morgan, Comp Mat Science **83**, p. 362 (2014).

[26] N. Galamba and B. C. Cabral, J. Chem Phys **126**, p. 24502 (2007).
[27] S. Clark, M. Segall, C. Pickard, P. Hasnip, M. Probert, K. Refson, and M. Payne, Z Kristallogr **220**, p. 567 (2005).
[28] A. Rappe, K. Rabe, E. Kaxiras, and J. Joannopoulos, Phys. Rev. B **41**, p. 1227 (1990).
[29] J. P. Perdew, K. Burke, and M. Ernzerhof, Phys. Rev. Lett. **77**, p. 3865 (1996).
[30] J. Hansen and I. McDonald, *Theory of simple liquids* (Academic Press, London, 2006).
[31] G. Kneller, V. Keiner, M. Kneller, and M. Schiller, Comput. Phys. Comm. **91**, p. 191 (1995).
[32] M. Telling and K. Andersen, Phys Chem Chem Phys **7**, p. 1255 (2005).
[33] V. F. Sears, Neutron News **3**, p. 29 (1992).
[34] G. Janz, *Molten Salts Handbook* (Academic Press, New York, 1967).
[35] S. Mukhopadhyay, P. Sushko, A. Stoneham, and A. Shluger, Phys. Rev. B **70**, p. 195203 (2004).
[36] F. Edwards, J. Enderby, R. Howe, and D. Page, J. Phys. C **8**, p. 3483 (1975).
[37] S. Biggin and J. Enderby, J. Phys. C **15**, p. L305 (1982).
[38] R. McGreevy and L. Pusztai, Proc Roy Soc A **430**, p. 241 (1990).
[39] X. Lv, Z. Xu, J. Li, J. Chen, and Q. Lu, J. Fluorine Chem. **185**, p. 42 (2016).
[40] G. L. Squires, *Introduction to the Theory of Thermal Neutron Scattering* (Cambridge University Press, Cambridge, UK, 2012).
[41] P. A. Egelstaff, *An Introduction to the Liquid State* (Clarendon Press, Oxford, UK, 1992).
[42] A. Karo and J. Hardy, Phys. Rev. **181**, p. 1272 (1969).
[43] F. Demmel, S. Hosokawa, M. Lorenzen, and W.-C. Pilgrim, Phys. Rev. B **69**, p. 12203 (2004).
[44] F. Demmel, D. Szubrin, W. Pilgrim, A. D. Francesco, and F. Formisano, Phys. Rev. E **92**, p. 12307 (2015).